




Research Article

Oxidase-Like Catalytic Performance of Nano-MnO₂ and Its Potential Application for Metal Ions Detection in Water

Kai Sun ¹, Qingzhu Liu,¹ Rui Zhu,¹ Qi Liu,¹ Shun Yao Li,² Youbin Si ¹
and Qingguo Huang ³

¹Anhui Province Key Laboratory of Farmland Ecological Conservation and Pollution Prevention,
School of Resources and Environment, Anhui Agricultural University, 130 Changjiang West Road, Hefei, 230036 Anhui, China

²College of Resources and Environmental Sciences, Nanjing Agricultural University, Nanjing 210095, China

³Department of Crop and Soil Sciences, University of Georgia, Griffin, GA 30223, USA

Correspondence should be addressed to Youbin Si; youbinsi@ahau.edu.cn and Qingguo Huang; qhuang@uga.edu

Received 3 June 2019; Revised 15 August 2019; Accepted 5 September 2019; Published 3 November 2019

Academic Editor: Günther K. Bonn

Copyright © 2019 Kai Sun et al. This is an open access article distributed under the Creative Commons Attribution License, which permits unrestricted use, distribution, and reproduction in any medium, provided the original work is properly cited.

Certain nano-scale metal oxides exhibiting the intrinsic enzyme-like reactivity had been used for environment monitoring. Herein, we evaluated the oxidase-mimicking activity of environmentally relevant nano-MnO₂ and its sensitivity to the presence of metal ions, and particularly, the use of MnO₂ nanozyme to potentially detect Cu²⁺, Zn²⁺, Mn²⁺, and Fe²⁺ in water. The results indicated the oxidase-like activity of nano-MnO₂ at acidic pH-driven oxidation of 2,6-dimethoxyphenol (2,6-DMP) via a single-electron transfer process, leading to the formation of a yellow product. Notably, the presence of Cu²⁺ and Mn²⁺ heightened the oxidase-mimicking activity of nano-MnO₂ at 25°C and pH 3.8, showing that Cu²⁺ and Mn²⁺ could modify the reactive sites of nano-MnO₂ surface to ameliorate its catalytic activity, while the activity of MnO₂ nanozyme in systems with Zn²⁺ and Fe²⁺ was impeded probably because of the strong affinity of Zn²⁺ and Fe²⁺ toward nano-MnO₂ surface. Based on these effects, we designed a procedure to use MnO₂ nanozyme to, respectively, detect Cu²⁺, Zn²⁺, Mn²⁺, and Fe²⁺ in the real water samples. MnO₂ nanozyme-based detecting systems achieved high accuracy (relative errors: 2.2–26.1%) and recovery (93.0–124.0%) for detection of the four metal ions, respectively. Such cost-effective detecting systems may provide a potential application for quantitative determination of metal ions in real water environmental samples.

1. Introduction

In recent years, considerable attention has been paid to the applications of artificial nanomaterials as nanozymes in mimicking the intrinsic catalytic function of natural enzymes due to their unique structural, electrical, and optical properties, as well as remarkable catalytic activities [1–3]. Compared with the natural enzymes, the artificial nanozymes exhibited higher robustness and stability under harsh conditions, lower production cost, simpler storage conditions, and more effective catalytic activity [4–6]. At present, nanozymes are primarily composed of artificial metal and metal oxide nanomaterials that can mimic the catalytic activities of natural peroxidases and/or oxidases [3, 7]. For instance, the intrinsic peroxidase-/oxidase-like activities of Au-Ag, CeO₂, MnFe₂O₄, NiO, and V₂O₅ nanoparticles have

been used in various applications ranging from biosensing and immunoassay to environment monitoring [3, 7–10]. Liu et al. reported the oxidase-mimicking activity of CeO₂ nanoparticles by fluoride capping, such nanozymes could detect micromolar levels of F⁻ in water and toothpastes [11].

It is well documented that MnO₂ nanomaterial had the intrinsic enzyme-like activity to catalyze the chromogenic reaction of substrates, which could be used as a nanozyme indicator for bioimaging, biosensing, and delivery of single-stranded DNA and drugs [3, 12, 13]. In particular, chromogenic reactions by nano-MnO₂ have been developed using dissolved O₂ as the oxidant, avoiding the use of H₂O₂ [14], thus providing easy and rapid detecting systems for quantitative analysis of any substances that can serve either as the accelerator or inhibitor of the chromogenic reactions [15, 16]. Such systems could be used for real environmental

water samples, but their potential application for quantitative determination of metal ions has been rarely explored.

The contamination of metal ions has always been a focus of concern [17]. Toxic metal ions (such as Cu^{2+} , Zn^{2+} , Pb^{2+} , and Fe^{2+}) having toxicity level greater than safety levels can cause acute toxicities to most aquatic biota [18]. Thus, having ways that can easily and rapidly detect these metal ions in water matrices is vital to protect wild species and human health. An instrumental method can be used to directly detect these metal ions in water samples, such as inductively coupled plasma mass spectrometry (ICPMS), but such methods are usually expensive and time-consuming and require expertise to operate [19, 20].

Recently, the enzyme-like activity of environmentally relevant nano- MnO_2 has proven to be highly effective for sensing applications [16, 21, 22]. In this study, nano- MnO_2 was chosen as the natural oxidase mimic owing to its outstanding redox chemistry, stability, and biocompatibility properties [23–25]. We systematically evaluated the oxidase-like activity of nano- MnO_2 in catalyzing the chromogenic reaction of 2,6-dimethoxyphenol (2,6-DMP), and identified the influence of Cu^{2+} , Zn^{2+} , Mn^{2+} , and Fe^{2+} , based on which methods were developed to, respectively, detect these metal ions in environmental water samples using MnO_2 nanozyme-2,6-DMP detecting systems.

2. Materials and Methods

2.1. Chemicals and Materials. Nano-scale MnO_2 ($\geq 99.9\%$) was obtained from DK Nano Technology Co., Ltd. (Beijing, China). The characteristics of nano- MnO_2 are shown in Figure 1. The size and morphology of the nano- MnO_2 were analyzed using a transmission electron microscope (TEM, JEM-200CX). The spectral characteristics of nano- MnO_2 were investigated using a UV-Vis spectroscope (Shimadzu, UV-2550) and a Fourier-transform infrared spectroscope (Thermo Scientific, NICOLET iS50 FTIR). The phase of the nano- MnO_2 was measured over the 2θ range from 5 to 85 degrees using an X-ray diffractometer (XRD, Thermo X'TRA).

2,6-DMP (CAS: 91-10-1) was purchased from Energy Chemical Technology Co., Ltd (Shanghai, China). Metal sulfates (*i.e.*, MgSO_4 , CuSO_4 , $\text{Al}_2(\text{SO}_4)_3$, ZnSO_4 , $\text{MnSO}_4 \cdot \text{H}_2\text{O}$, $\text{FeSO}_4 \cdot 7\text{H}_2\text{O}$, and PbSO_4) were obtained from Shanghai Aladdin Bio-Chem Technology Co., Ltd. Stock solutions of metal ions ($100 \text{ mmol} \cdot \text{L}^{-1}$) were prepared in Milli-Q ultrapure water ($18.2 \text{ M}\Omega \cdot \text{cm}$) and stored at 4°C . We had previously evaluated the effects of K^+ , Na^+ , Ag^+ , Co^{2+} , Hg^{2+} , Ca^{2+} , Cd^{2+} , and Fe^{3+} on the oxidase-like activity of nano- MnO_2 . The buffer used in this study was a citrate-phosphate buffer solution (C-PBS: $10 \text{ mmol} \cdot \text{L}^{-1}$ citric acid and $10 \text{ mmol} \cdot \text{L}^{-1}$ Na_2HPO_4 , pH 3.8) adjusted with HCl and NaOH. All the other chemicals were of analytical reagent grade and used as received.

2.2. Assessment of the Enzyme-Like Activity of Nano- MnO_2 . To assess the enzyme-like activity of nano- MnO_2 , MnO_2 nanoparticles were tested in 10 mL of a C-PBS ($10 \text{ mmol} \cdot \text{L}^{-1}$,

pH 3.8) buffer at room temperature (25°C) containing $1.0 \text{ mmol} \cdot \text{L}^{-1}$ 2,6-DMP as the chromogenic substrate and naturally dissolved O_2 as the cofactor [14, 26]. After the nano- MnO_2 ($0.1 \text{ mg} \cdot \text{mL}^{-1}$) had been mixed thoroughly with the 2,6-DMP reaction solution, the absorbance was immediately measured at 468 nm using a UV-Vis spectrophotometer (Shanghai Lengguang 722S) in a quartz cuvette with a 1 cm light path. The solution was monitored every 20 s for 3 min by recording the change of absorbance value at 468 nm. One unit of nano- MnO_2 activity ($\text{U} \cdot \text{mL}^{-1}$) is defined as the amount of nanozyme that causes one unit of absorbance change per minute at 468 nm in C-PBS ($10 \text{ mmol} \cdot \text{L}^{-1}$, pH 3.8) buffer containing $1.0 \text{ mmol} \cdot \text{L}^{-1}$ 2,6-DMP. Therefore, the oxidase-mimicking activity of nano- MnO_2 can be calculated through the rate of absorbance change. The same solution free of nano- MnO_2 was used as the blank control. All experiments were performed in triplicate.

2.3. Effect of Different Factors on the Enzyme-Like Activity of Nano- MnO_2 . To evaluate the influence of nano- MnO_2 dosage on 2,6-DMP oxidation, the reaction was conducted in a 50 mL flask containing $1.0 \text{ mmol} \cdot \text{L}^{-1}$ 2,6-DMP and nano- MnO_2 varying between 0.005 and $0.32 \text{ mg} \cdot \text{mL}^{-1}$ in 10 mL C-PBS ($10 \text{ mmol} \cdot \text{L}^{-1}$) at 25°C and pH 3.8. The effect of the substrate concentration on the chromogenic reaction was also performed in a 50 mL flask containing $0.1 \text{ mg} \cdot \text{mL}^{-1}$ nano- MnO_2 and 2,6-DMP at a concentration varying between 0.005 and $1.0 \text{ mmol} \cdot \text{L}^{-1}$ in 10 mL C-PBS. The reaction kinetics parameters K_m and v_{max} were calculated by the Lineweaver–Burk plot of the Michaelis–Menten kinetics equation:

$$\frac{1}{v} = \left(\frac{K_m + [S]}{v_{\text{max}} \cdot [S]} \right), \quad (1)$$

where v is the reaction velocity, $[S]$ is the substrate concentration, K_m is the Michaelis constant, and v_{max} is the maximal reaction velocity.

Experimental procedures similar to those described above were used to explore the effects of pH and temperature on the enzyme-like activity of nano- MnO_2 . The reactions were carried at different pH and a wide range of temperature. For studying the pH effect, 10 mL of $10 \text{ mmol} \cdot \text{L}^{-1}$ C-PBS (pH 2.0–10.0) buffer containing $1.0 \text{ mmol} \cdot \text{L}^{-1}$ 2,6-DMP was mixed with $0.1 \text{ mg} \cdot \text{mL}^{-1}$ nano- MnO_2 at room temperature (25°C). For studying the effect of temperature, 10 mL of $10 \text{ mmol} \cdot \text{L}^{-1}$ C-PBS (pH 3.8) buffer containing $1.0 \text{ mmol} \cdot \text{L}^{-1}$ 2,6-DMP was mixed with $0.1 \text{ mg} \cdot \text{mL}^{-1}$ nano- MnO_2 at a temperature ranging from 10°C to 90°C . Absorbance was recorded at 468 nm at 20 s intervals. All experiments were performed in triplicate.

2.4. Enzyme-Like Activity of Nano- MnO_2 for Detecting Metal Ions in Water. A series of mixtures containing different metal ions (*i.e.*, Mg^{2+} , Cu^{2+} , Al^{3+} , Zn^{2+} , Mn^{2+} , Fe^{2+} , and Pb^{2+}) and nano- MnO_2 ($0.1 \text{ mg} \cdot \text{mL}^{-1}$) in 10 mL of C-PBS buffer (pH 3.8) were equilibrated at room temperature

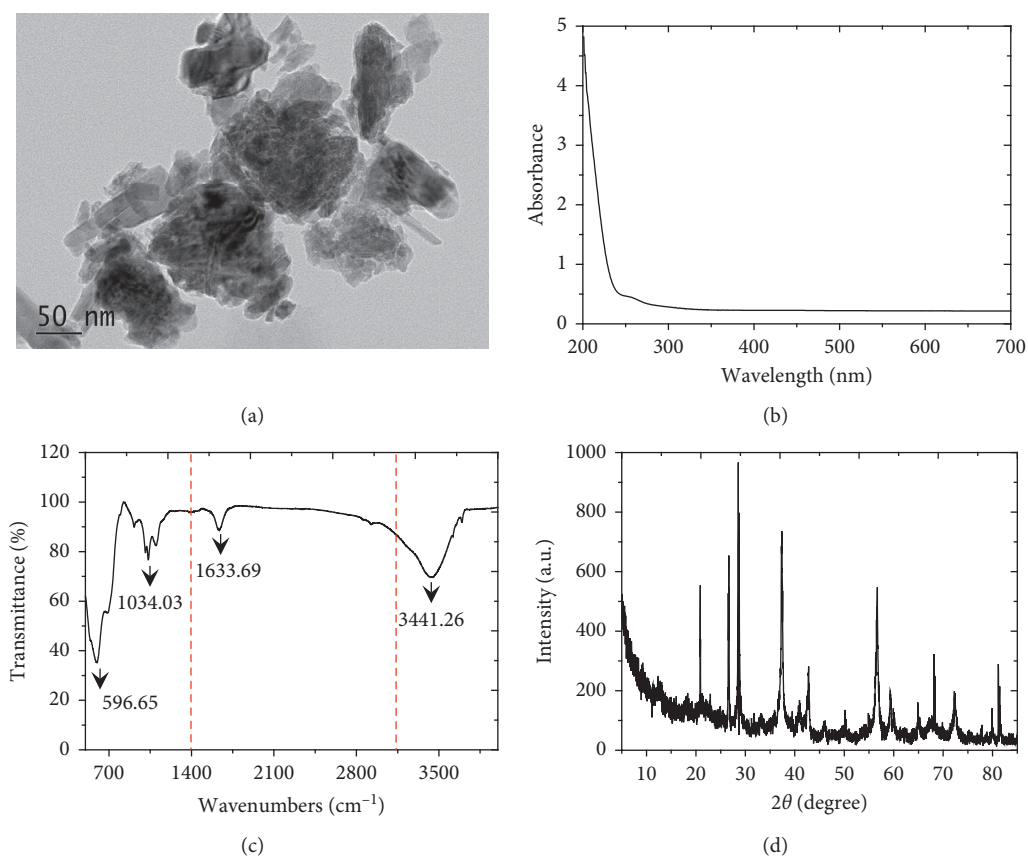


FIGURE 1: MnO_2 nanomaterial was characterized by (a) TEM imaging, (b) UV-Vis spectra, (c) FTIR spectra, and (d) XRD pattern to determine the size, morphology, group, and crystalline structure of nano- MnO_2 .

(25°C), and then C-PBS containing $1.0 \text{ mmol}\cdot\text{L}^{-1}$ 2,6-DMP was added to each of the mixtures and then monitored using a UV-Vis spectrophotometer at 468 nm. All experiments were performed in triplicate.

Based on the above results, MnO_2 nanozyme-2,6-DMP reaction systems for, respectively, detecting Cu^{2+} , Zn^{2+} , Mn^{2+} , and Fe^{2+} in real environmental water matrices were also assessed. 10-fold dilution of real samples (pond water 1 and 2 from Anhui Agricultural University campus) in C-PBS buffer ($10 \text{ mmol}\cdot\text{L}^{-1}$, pH 3.8) were spiked with Cu^{2+} , Zn^{2+} , Mn^{2+} , or Fe^{2+} (0.002 , 0.01 , 0.05 , and $0.25 \text{ mmol}\cdot\text{L}^{-1}$) and were then detected using the described MnO_2 nanozyme-2,6-DMP-sensing systems following the same process described above. Additionally, these samples were also determined by ICPMS (6300 Series, Thermo Fourier, USA) for comparison. All experiments were performed in quintuplicate.

2.5. Statistical Analysis. All data were processed with Excel 2010 (Microsoft, Redmond, WA). Each data point in the figures and tables represents an average value. The standard deviation of replicate samples is shown in the figures as an error bar.

3. Results and Discussions

3.1. Oxidase-Like Activity of Nano- MnO_2 . To assess the intrinsic enzyme-mimicking activity of nano- MnO_2 , 2,6-DMP

was chosen as the chromogenic substrate in the standard oxidation reaction, and the reaction kinetics was tested at 468 nm corresponding to the oxidized 2,6-DMP. The change of absorbance over time by the oxidation of 2,6-DMP in C-PBS buffer at 25°C and pH 3.8 is shown in Figure 2. Nano- MnO_2 could catalyze the colorless 2,6-DMP to form a chromogenic product (a yellow product, *i.e.*, 3,3',5,5'-tetramethyl-4,4'-diphenquinone) with a change in absorbance via the radical-based C-C self-coupling mechanism, like laccase-mediated oxidative coupling reactions of 2,6-DMP under the same conditions [26, 27]. The absorbance changes linearly with time under the tested conditions ($R^2 > 0.99$), and the oxidase-like activity of nano- MnO_2 was calculated to be $0.047 \text{ U}\cdot\text{mL}^{-1}$. The oxidative coupling of 2,6-DMP catalyzed by nano- MnO_2 was described as follows: first, 2,6-DMP was adsorbed onto the reactive sites of nano- MnO_2 surface, followed by the single-electron oxidation of 2,6-DMP by nano- MnO_2 , leading to the formation of chromogenic product and the release of Mn^{2+} from the nanoparticle surface [14, 28].

The role of dissolved O_2 in the oxidation of 2,6-DMP was evaluated by purging the reaction solution with N_2 , resulting in a decrease on the oxidase-like activity of nano- MnO_2 . This revealed that dissolved O_2 acted as an electron acceptor in the catalytic reactions [14, 29]. This result is in agreement with an earlier report that indicated the oxidation of a substrate in the absence of H_2O_2 via bovine

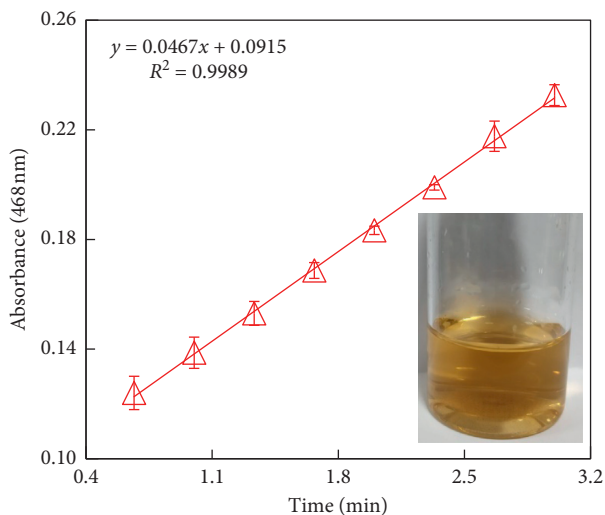


FIGURE 2: Oxidase-like activity of nano-MnO₂ for catalyzing the chromogenic reaction of 2,6-DMP in C-PBS buffer at 25°C and pH 3.8. Reaction conditions: Nano-MnO₂ = 0.1 mg·mL⁻¹; 2,6-DMP = 1.0 mmol·L⁻¹. Error bars represent the standard deviation ($n = 3$).

serum albumin- (BSA-) stabilized MnO₂ nanoparticles [30]. Additionally, the stability of nano-MnO₂ in the reaction system was also studied over a one-month storage period. With the increase in storage time, the release of Mn²⁺ increased mildly, but no significant difference in the oxidation of 2,6-DMP was detected, implying that the capacity of nano-MnO₂ to oxidize 2,6-DMP exhibits a high stability. These results demonstrated that nano-MnO₂ possessed a stable oxidase-like activity to catalyze the chromogenic reaction of 2,6-DMP at 25°C and pH 3.8 in the absence of H₂O₂.

3.2. Effects of Nano-MnO₂ and Substrate Concentration on 2,6-DMP Oxidation. We further assessed the influence of nano-MnO₂ concentration on 2,6-DMP oxidation catalyzed by MnO₂ nanozyme by UV-Vis spectrophotometry. As shown in Figure 3, the oxidation of 2,6-DMP catalyzed by MnO₂ nanozyme showed a distinct absorbance peak at the wavelength of 468 nm, and the increase of this absorbance over time was obvious resulting from 2,6-DMP oxidation (Figure 2). The variation of the absorbance peak was observed by adding different concentrations of MnO₂ nanozyme (Figure 3). Increasing the concentration of nano-MnO₂ from 0.005 to 0.3 mg·mL⁻¹ resulted in a liner increase in the oxidase-like activity of nano-MnO₂ (0.002–0.126 U·mL⁻¹) in oxidizing 2,6-DMP (Figure 4). According to the correlation of the nano-MnO₂ concentration and its oxidase-like activity, the apparent pseudo-second-order rate constant was determined to be 0.445 U·mg⁻¹ ($R^2 = 0.992$). These results demonstrated that increasing the concentration of nano-MnO₂ facilitated the oxidase-like activity of nano-MnO₂ to catalyze the oxidation of 2,6-DMP.

For discussing the catalytic mechanism and obtaining the steady-state kinetic parameters, the initial reaction rate (1 min) of 2,6-DMP oxidation catalyzed by nano-MnO₂ was

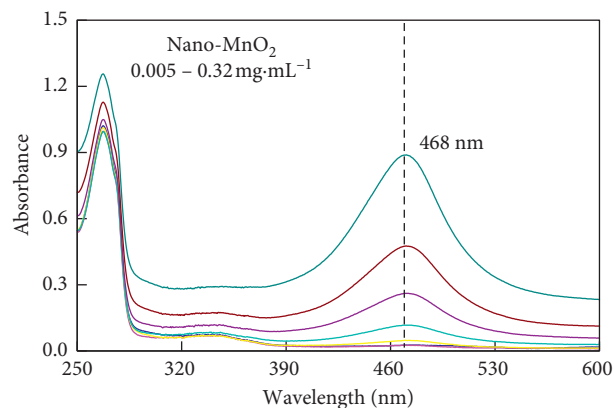


FIGURE 3: UV-Vis absorption spectra of 2,6-DMP reacted with different nano-MnO₂ concentrations at the wavelength of 250–600 nm. Reaction conditions: Nano-MnO₂ = 0.005–0.32 mg·mL⁻¹; 2,6-DMP = 1.0 mmol·L⁻¹.

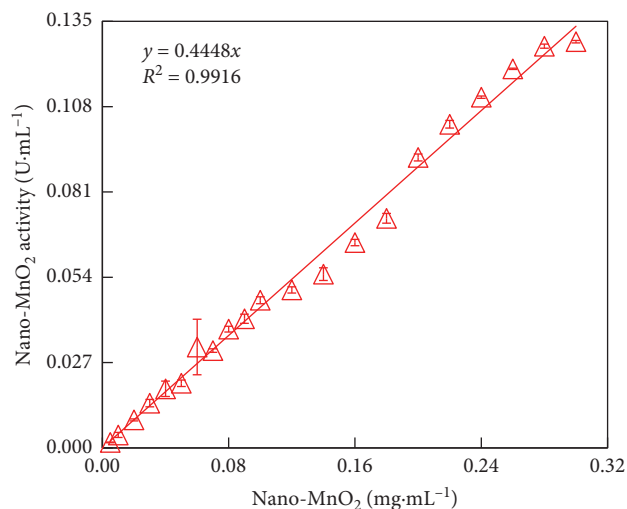


FIGURE 4: Concentration-dependent kinetic study of the oxidase-like activity of nano-MnO₂ for a 3 min reaction. Reaction conditions: [Nano-MnO₂] = 0.005–0.3 mg·mL⁻¹, [2,6-DMP] = 1.0 mmol·L⁻¹. Error bars represent the standard deviation ($n = 3$).

investigated with the initial 2,6-DMP concentration varying between 0.005 and 0.2 mmol·L⁻¹. A hyperbolic relationship between the substrate concentration and the rate of reaction (v) was revealed in Figure 5(a), like the typical Michaelis-Menten curve. The apparent enzyme kinetic parameters such as K_m and v_{max} values could be calculated by Lineweaver-Burk plot (Figure 5(b)). From the kinetic analysis, it was found that MnO₂ nanozyme showed a high affinity towards 2,6-DMP. The K_m and v_{max} values were 0.005 and 0.155 ($R^2 = 0.999$), respectively. Combining with previous studies on artificial metal oxide-based nanozymes [24, 31, 32], MnO₂ nanoparticles are promising nanomimetics for oxidase. It is noted that the oxidase-like activity of nano-MnO₂ and the steady-state kinetic parameter values were investigated at an acidic pH (pH 3.8) because of its limited oxidase-like activity at physiological or basic pH.

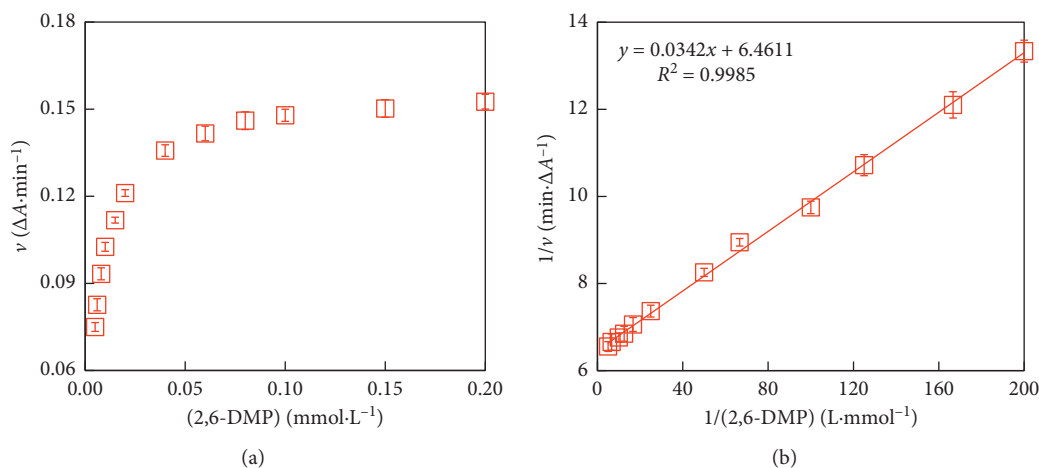


FIGURE 5: Studies of kinetic reaction parameters K_m and v_{max} . (a) The Michaelis–Menten curve for the oxidase-like activity of nano-MnO₂. (b) Lineweaver–Burk plot of 2,6-DMP oxidation was made from the Michaelis–Menten curve. Reaction conditions: NaO-MnO₂ = 0.1 mg·mL⁻¹; 2,6-DMP = 0.005–0.2 mmol·L⁻¹. Error bars represent the standard deviation ($n = 3$).

3.3. Effects of pH and Temperature on 2,6-DMP Oxidation.

Similar to the natural oxidase, the catalytic activity of MnO₂ nanozyme is also dependent on pH and temperature. As shown in Figure 6, the catalytic activity of MnO₂ nanozyme decreased with the rise of reaction pH from 2.0 to 7.0, whereas the oxidase-like activity of MnO₂ nanozyme increased with the rise of reaction temperature from 10°C to 90°C. It was found that only 0.022 U·mL⁻¹ of nano-MnO₂ activity was retained at pH 7.0, while 0.205 U·mL⁻¹ of activity was retained even at 90°C. As the reaction pH increasing from 7.0 to 10.0, the oxidase-like activity of nano-MnO₂ had not exhibited an obvious variation. As the temperature increased from 10°C to 25°C, the catalytic activity of nano-MnO₂ was mildly enhanced. It was noted that as the temperature increased from 30°C to 90°C, the catalytic activity rapidly increased. Temperature varying in the range of 10–25°C had little impact on the final colorimetric signal. Change in pH and temperature had not resulted in inactivation of MnO₂ nanozyme. These results indicated that the oxidase-like activity of nano-MnO₂ exhibited a wide range of pH and thermal stability, unlike the natural oxidase [33, 34].

3.4. Metal Ions Induced the Effect of MnO₂ Nanozyme Activity.

Simply and accurately detecting metal ions is of great significance in the aqueous environment. Several nanozymes had been used to detect metal ions (*i.e.*, Hg²⁺ and Pb²⁺) due to their intrinsic advantages and high stability under harsh conditions [35–37]. In this study, the selectivity of MnO₂ nanozyme activity was evaluated in the presence of various metal ions including Mg²⁺, Cu²⁺, Al³⁺, Zn²⁺, Mn²⁺, Fe²⁺, and Pb²⁺ in 10 mL C-PBS buffer at 25°C and pH 3.8. As shown in Figure 7, the oxidase-like activity of nano-MnO₂ was 0.045 U·mL⁻¹ in the blank control (BC, *i.e.*, metal ion-free) samples. Compared with BC, the activity of MnO₂ nanozyme was significantly enhanced in the presence of Cu²⁺ and Mn²⁺ ($P < 0.01$), whereas the presence of Zn²⁺ and Fe²⁺ obviously suppressed the activity of MnO₂ nanozyme ($P < 0.05$). Interestingly, there was no significant

interference on the activity of MnO₂ nanozyme in aqueous solution by other metal ions. These results implied that MnO₂ nanozyme might be used to, respectively, detect Cu²⁺, Mn²⁺, Zn²⁺, and Fe²⁺ in aquatic environment. However, the selectivity of MnO₂ nanozyme toward Cu²⁺, Mn²⁺, Zn²⁺, and Fe²⁺ against other ions needs further studies due to the complexity of valence states of metal elements in the nanoparticles.

Previous studies had also indicated that certain metal ions could effectively upregulate/downregulate the activity of nanozymes through surface deposition and metallophilic interactions [38–40]. For MnO₂ nanozyme detecting systems, the substrate (2,6-DMP) was transformed into a chromogenic product, serving as a signal amplifier. The presence of Cu²⁺ and Mn²⁺ enhanced the activity of MnO₂ nanozyme, likely because these metal ions modified the reactive sites of nano-MnO₂ surface [41, 42]. First, Cu²⁺ and/or Mn²⁺ ions reacted with citrate to form metal ion-citrate complex, subsequently the complex dispersed onto the surface of nano-MnO₂, and thus changed the surface properties of nano-MnO₂, thereby enhancing its oxidase-like activity [43, 44]. On the contrary, the suppressive activity on MnO₂ nanozyme in the presence of Zn²⁺ and Fe²⁺ occurred probably owing to the strong affinity of Zn²⁺ and Fe²⁺ toward the nano-MnO₂ surface via the electrostatic attractions or metal ion-multivalent Mn interactions [36, 39, 40]. The binding affinity of MnO₂ nanozyme for Zn²⁺ and Fe²⁺ was very high. The adsorption of Zn²⁺ and Fe²⁺ onto the MnO₂ nanozyme impeded the electron transfer to 2,6-DMP, thus diminishing the oxidase-like activity of nano-MnO₂ [39]. Additionally, the control samples free of MnO₂ nanozyme with the metal ion present did not show the oxidase-like activity towards O₂-2,6-DMP during the incubation period.

3.5. MnO₂ Nanozyme-Based Reaction Systems for Detecting Cu²⁺, Zn²⁺, Mn²⁺, or Fe²⁺.

As shown in Figure 8, MnO₂ nanozyme-sensing systems were carried out by, respectively,

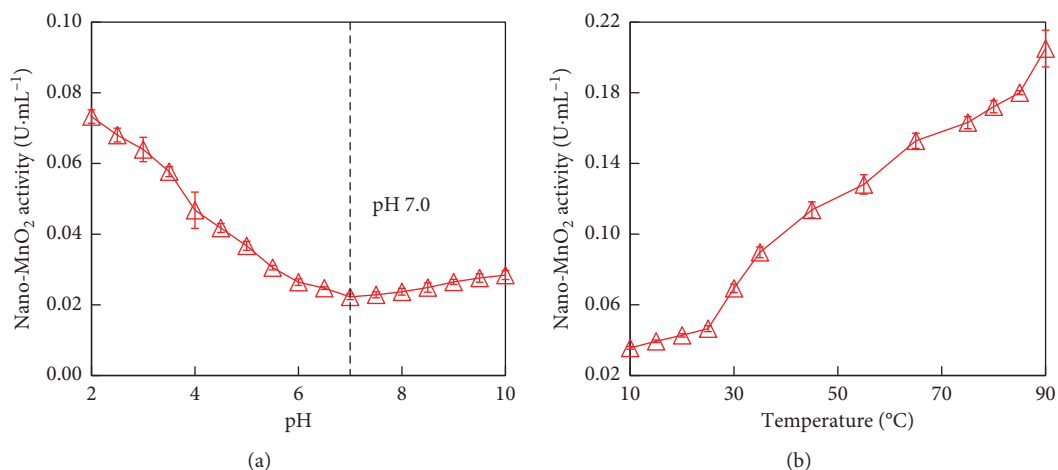


FIGURE 6: pH and temperature dependent the oxidase-like activity of nano-MnO₂ for catalyzing the oxidation of 2,6-DMP. (a) Reaction conditions: Nano-MnO₂ = 0.1 mg·mL⁻¹; 2,6-DMP = 1.0 mmol·L⁻¹, pH 2.0–10.0. (b) Reaction conditions: Nano-MnO₂ = 0.1 mg·mL⁻¹; 2,6-DMP = 1.0 mmol·L⁻¹; Temperature = 10–90°C. Error bars represent the standard deviation ($n = 3$).

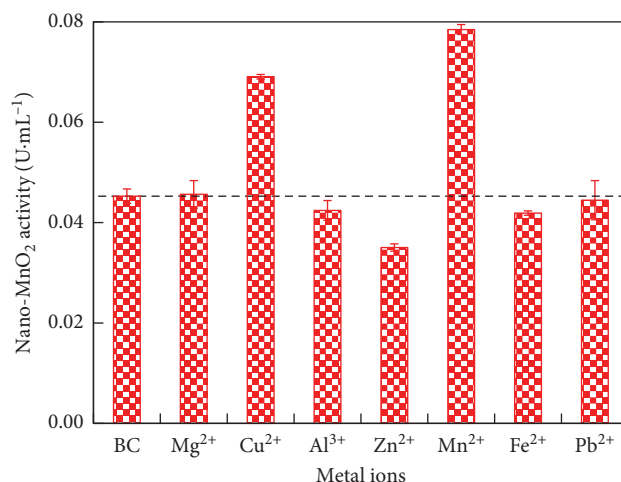


FIGURE 7: Role of metal ions (*i.e.*, Mg²⁺, Cu²⁺, Al³⁺, Zn²⁺, Mn²⁺, Fe²⁺, and Pb²⁺) on the oxidase-like activity of nano-MnO₂ for catalyzing the oxidation of 2,6-DMP. Reaction conditions: Nano-MnO₂ = 0.1 mg·mL⁻¹; 2,6-DMP = 1.0 mmol·L⁻¹; Metal ion = 0.01 mmol·L⁻¹. Error bars represent the standard deviation ($n = 3$).

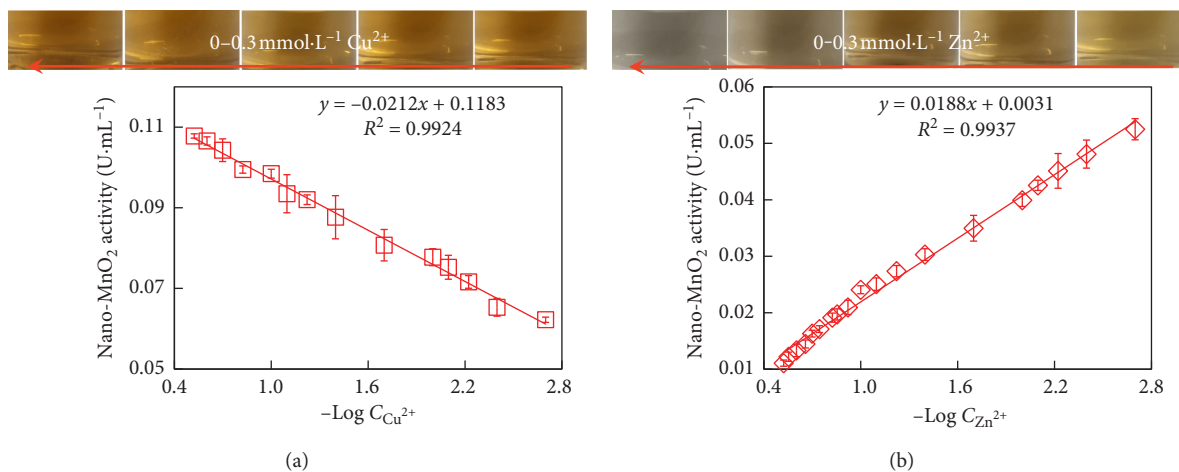


FIGURE 8: Continued.

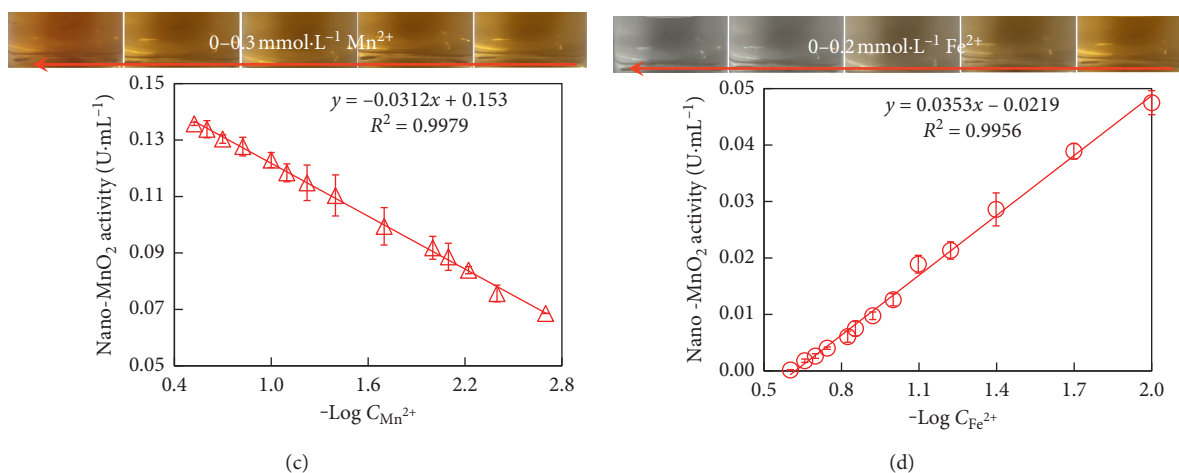


FIGURE 8: Linear correlation between the oxidase-like activity of nano-MnO₂ and the logarithmic value of metal ion concentration (Log C). Reaction conditions: Nano-MnO₂ = 0.1 mg·mL⁻¹; 2,6-DMP = 1.0 mmol·L⁻¹; Metal ion = 0.002–0.3 mmol·L⁻¹. Error bars represent the standard deviation ($n = 3$).

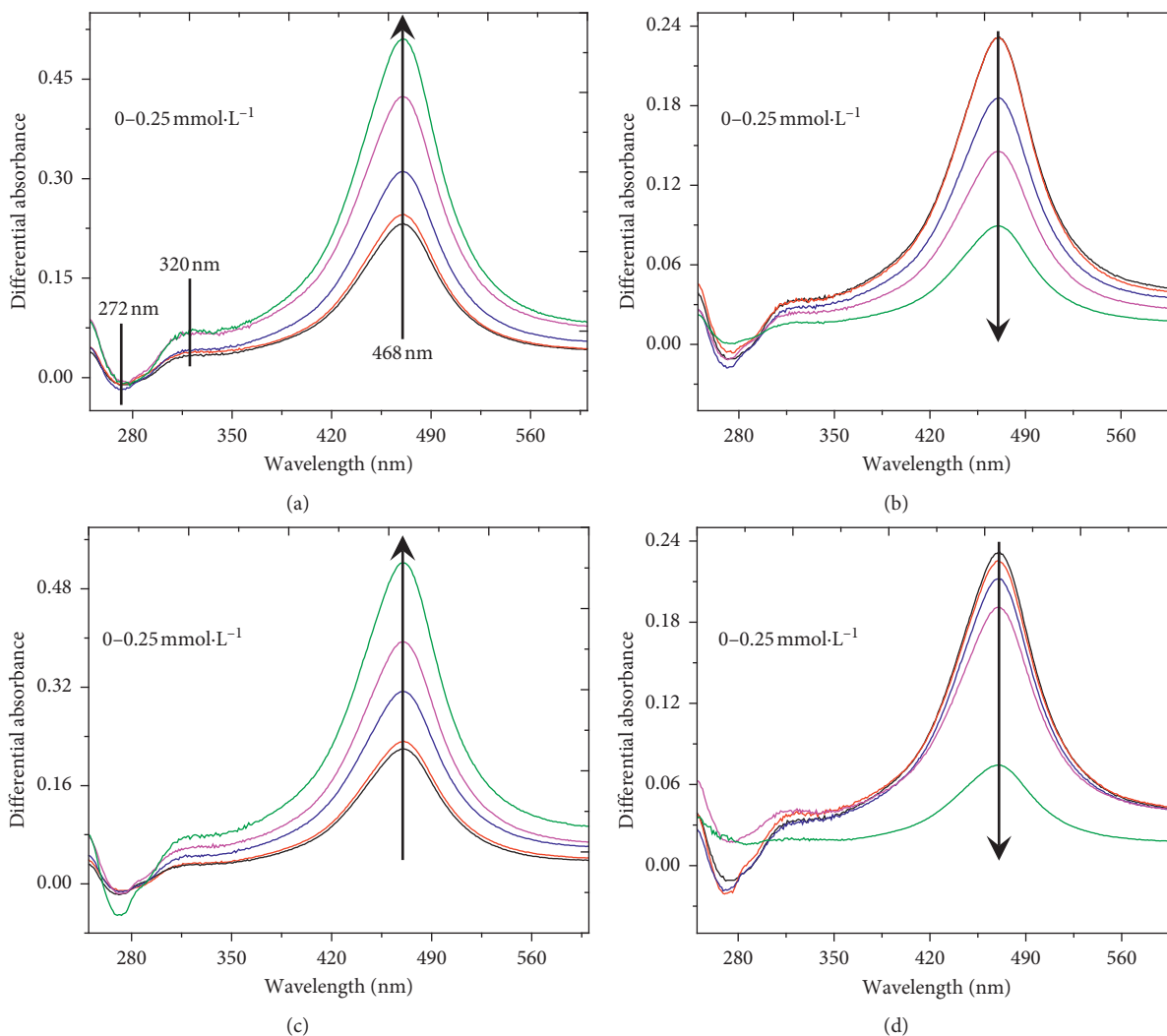


FIGURE 9: UV-Vis differential absorbance spectra (DAS) calculated on the basis of the data recorded at different metal ion concentrations (0, 0.002, 0.01, 0.05, and 0.25 mmol·L⁻¹). Reaction conditions: Nano-MnO₂ = 0.1 mg·mL⁻¹; 2,6-DMP = 1.0 mmol·L⁻¹; metal ion = 0–0.25 mmol·L⁻¹. Error bars represent the standard deviation ($n = 3$). (a) Cu²⁺, (b) Zn²⁺, (c) Mn²⁺, and (d) Fe²⁺.

TABLE 1: Analytical results for the detection of metal ion-contaminated water samples by MnO₂ nanozyme-2,6-DMP detecting systems.

Real samples	Added Cu ²⁺ (mmol·L ⁻¹)	Detected Cu ²⁺ (mmol·L ⁻¹)	Recovery	RSD (n = 5)	Added Zn ²⁺ (mmol·L ⁻¹)	Detected Zn ²⁺ (mmol·L ⁻¹)	Recovery	RSD (n = 5)	Added Mn ²⁺ (mmol·L ⁻¹)	Detected Mn ²⁺ (mmol·L ⁻¹)	Recovery	RSD (n = 5)	Added Fe ²⁺ (mmol·L ⁻¹)	Detected Fe ²⁺ (mmol·L ⁻¹)	Recovery	RSD (n = 5)
Pond water 1	0.002	0.002	104.8%	6.9%	0.002	0.002	108.6%	7.3%	0.002	0.002	106.7%	5.4%	0.002	0.002	116.5%	13.2%
	0.01	0.010	101.1%	3.7%	0.01	0.013	111.2%	10.5%	0.01	0.009	98.6%	6.3%	0.01	0.011	114.9%	8.8%
	0.05	0.052	105.8%	5.4%	0.05	0.051	102.7%	3.8%	0.05	0.053	106.1%	7.4%	0.05	0.056	111.9%	26.1%
	0.25	0.253	106.6%	4.9%	0.25	0.0248	97.8%	4.3%	0.25	0.255	112.4%	11.2%	0.25	0.246	96.6%	12.0%
Pond water 2	0.002	0.002	106.9%	9.8%	0.002	0.002	95.0%	6.7%	0.002	0.002	106.5%	6.3%	0.002	0.002	110.5%	15.7%
	0.01	0.009	93.0%	11.2%	0.01	0.013	111.2%	5.3%	0.01	0.012	124.0%	11.8%	0.01	0.011	114.3%	8.6%
	0.05	0.054	108.6%	7.6%	0.05	0.052	104.4%	4.2%	0.05	0.047	94.5%	4.9%	0.05	0.048	97.2%	7.3%
	0.25	0.248	99.4%	3.3%	0.25	0.246	98.5%	3.1%	0.25	0.254	101.7%	2.2%	0.25	0.252	100.9%	3.5%

detecting Cu^{2+} , Zn^{2+} , Mn^{2+} , and Fe^{2+} in a concentration range of $0.002\text{--}0.3\text{ mmol}\cdot\text{L}^{-1}$ by the change of MnO_2 nanozyme activity in the presence of these metal ions. It was noted that increasing the concentrations of Cu^{2+} and Mn^{2+} resulted in a color progression from yellow to deep yellow, while increasing the concentrations of Zn^{2+} and Fe^{2+} resulted in a color progression from yellow to colorless. A linear correlation between the activities of MnO_2 nanozyme and the logarithmic values of metal ions concentration ($0.002\text{--}0.3\text{ mmol}\cdot\text{L}^{-1}$) was observed (Figure 8). The activity of MnO_2 nanozyme increased with increasing Cu^{2+} and Mn^{2+} concentrations, whereas the activity of MnO_2 nanozyme decreased with increasing the concentrations of Zn^{2+} and Fe^{2+} ions. The slopes of the linear regression for the four metal ions (*i.e.*, Cu^{2+} , Zn^{2+} , Mn^{2+} , and Fe^{2+}) were -0.021 , 0.019 , -0.031 , and 0.035 , respectively. MnO_2 nanozyme-2,6-DMP-sensing systems showed high sensitivity and a wide dynamic range for, respectively, detection of Cu^{2+} , Zn^{2+} , Mn^{2+} , and Fe^{2+} , allowing for a limit of detection less than $0.002\text{ mmol}\cdot\text{L}^{-1}$, which was lower than the maximum levels of Cu^{2+} , Zn^{2+} , Mn^{2+} , and Fe^{2+} (0.016 , 0.015 , 0.002 , and $0.005\text{ mmol}\cdot\text{L}^{-1}$, respectively) in drinking water permitted by the national standards GB 5749-2006 sanitary standard of China.

To further investigate the possible interaction mechanism between metal ions and MnO_2 nanozyme, a differential UV-Vis spectrometry approach was performed [45]. The differential absorbance spectrum (DAS) could be calculated by the following equation:

$$\Delta A_{\text{DAS}} = A_{\text{mixture}} - A_{2,6\text{-DMP}} - A_{\text{metal ion}}, \quad (2)$$

where A_{mixture} , $A_{2,6\text{-DMP}}$, and $A_{\text{metal ion}}$ are, respectively, the absorbance at $250\text{--}600\text{ nm}$ wavelength of the mixture solution, and the corresponding reference 2,6-DMP and metal ion solution.

As shown in Figure 9, the DAS of four reaction systems had an intensive negative peak at 272 nm and two intensive positive peaks, respectively, at 320 and 468 nm , implying that the change of electronic density in the molecules caused by the formation of a complex and/or metal ion-multivalent Mn interactions in C-PBS buffer. On the one hand, the formation of complex between $\text{Cu}^{2+}/\text{Mn}^{2+}$ and citrate changed the surface properties of MnO_2 nanozyme, thus facilitating its oxidase-like activity [43, 44, 46]. On the other hand, Zn^{2+} and Fe^{2+} were bound to the reactive sites of MnO_2 nanozyme surface, leading to the hindrance of electron transfer between the MnO_2 nanozyme and 2,6-DMP, consequently restraining the activity of MnO_2 nanozyme [39, 40].

3.6. Detection of Metal Ions in Real Water Samples. In order to verify the metal sensing ability of MnO_2 nanozyme for real environmental water samples, tests were performed with different concentrations of Cu^{2+} , Zn^{2+} , Mn^{2+} , or Fe^{2+} spiked to pond water samples 1 and 2 from Anhui Agricultural University. First, samples were diluted 10-fold with C-PBS buffer (pH 3.8) to minimize the matrix effect. Subsequently, Cu^{2+} , Zn^{2+} , Mn^{2+} , or Fe^{2+} at a concentration of $0.002\text{--}0.25\text{ mmol}\cdot\text{L}^{-1}$

were spiked to the pond water samples. As shown in Table 1, the recoveries were $93.0\text{--}124.0\%$ for $0.002\text{--}0.25\text{ mmol}\cdot\text{L}^{-1}$ metal ions (*i.e.*, Cu^{2+} , Zn^{2+} , Mn^{2+} , and Fe^{2+}) that were spiked to the pond water 1 and 2. The concentrations of Cu^{2+} , Zn^{2+} , Mn^{2+} , and Fe^{2+} in the pond water samples 1 and 2 were also determined by ICPMS, which did not show significant difference from that obtained by the MnO_2 nanozyme-detecting systems. In addition, the nanozyme-sensing method exhibited stable performance at a broad range of pH and temperature, convenient for experimental applications. It is noteworthy that the response of the MnO_2 nanozyme-sensing systems to Zn^{2+} and Fe^{2+} at high concentrations can be directly observed with the naked eye. These results confirmed that the MnO_2 nanozyme-2,6-DMP-sensing systems may be applicable to real water environmental samples for easily and rapidly quantifying Cu^{2+} , Zn^{2+} , Mn^{2+} , or Fe^{2+} . Even so, how to improve the selectivity of MnO_2 nanozyme for metal ions detection in water is still crucial. To achieve that, two of the following main issues need to be resolved. One is studying the catalytic performance and steady-state kinetics to uncover the interaction mechanism between MnO_2 nanozyme and metal ions, and the other is modifying the surface of MnO_2 nanozyme to improve its catalytic activity and environmental application in real water [3, 13, 44, 47, 48].

4. Conclusions

In this study, nano- MnO_2 was used as an oxidase mimetic to catalyze the chromogenic reaction of 2,6-DMP in C-PBS buffer. The results indicated that nano- MnO_2 possessed the oxidase-like activity with the K_m and v_{max} values of 0.005 and 0.155 ($R^2 = 0.999$), respectively, at 25°C and pH 3.8. Additionally, the effect of metal ions on this colorimetric reaction catalyzed by MnO_2 nanozyme was explored, based on which it was found that this reaction system could be used to, respectively, detect Cu^{2+} , Zn^{2+} , Mn^{2+} , and Fe^{2+} in aqueous solution without significant interference from other factors. The detection limit for the four metal ions was less than $0.002\text{ mmol}\cdot\text{L}^{-1}$ and the linear response range was $0.002\text{--}0.25\text{ mmol}\cdot\text{L}^{-1}$. Use of this detecting system was demonstrated with real environmental water samples, and the results indicated that the MnO_2 nanozyme-based sensing was simple and rapid for quantitative determination of Cu^{2+} , Zn^{2+} , Mn^{2+} , and Fe^{2+} . It is noted that MnO_2 nanozyme was unable to determine ultralow metal ion concentration; thus, a more sensitive detecting assay should be developed in the follow-up study.

Data Availability

The data used to support the findings of this study are available from the corresponding author upon request.

Conflicts of Interest

The authors declare no competing financial interests.

Acknowledgments

We are grateful to D. Xie and S. Wang for assistance with data collection. Research was supported by the National

Science Foundation of China (41907314) and the Natural Science Foundation of Anhui Province (1808085QD104).

References

- [1] M.-C. Daniel and D. Astruc, "Gold nanoparticles: assembly, supramolecular chemistry, quantum-size-related properties, and applications toward biology, catalysis, and nanotechnology," *Chemical Reviews*, vol. 104, no. 1, pp. 293–346, 2004.
- [2] Y. Lin, J. Ren, and X. Qu, "Catalytically active nanomaterials: a promising candidate for artificial enzymes," *Accounts of Chemical Research*, vol. 47, no. 4, pp. 1097–1105, 2014.
- [3] W. Chen, S. Li, J. Wang, K. Sun, and Y. Si, "Metal and metal oxide nanozymes: bioenzymatic characteristic, catalytic mechanism, and eco-environmental applications," *Nanoscale*, vol. 11, no. 34, pp. 15783–15793, 2019.
- [4] H. Y. Shin, T. J. Park, and M. I. Kim, "Recent research trends and future prospects in nanozymes," *Journal of Nanomaterials*, vol. 2015, Article ID 756278, 11 pages, 2015.
- [5] L. Han, P. Liu, H. Zhang, F. Li, and A. Liu, "Phage capsid protein-directed MnO₂ nanosheets with peroxidase-like activity for spectrometric biosensing and evaluation of anti-oxidant behaviour," *Chemical Communications*, vol. 53, no. 37, pp. 5216–5219, 2017.
- [6] L. Han, L. Zeng, M. Wei, C. M. Li, and A. Liu, "A V₂O₃-ordered mesoporous carbon composite with novel peroxidase-like activity towards the glucose colorimetric assay," *Nanoscale*, vol. 7, no. 27, pp. 11678–11685, 2015.
- [7] L. Han, C. Li, T. Zhang, Q. Lang, and A. Liu, "Au@Ag heterogeneous nanorods as nanozyme interfaces with peroxidase-like activity and their application for one-pot analysis of glucose at nearly neutral pH," *ACS Applied Materials & Interfaces*, vol. 7, no. 26, pp. 14463–14470, 2015.
- [8] X. Niu, K. Ye, Z. Li et al., "Pyrophosphate-mediated on-off-on oxidase-like activity switching of nanosized MnFe₂O₄ for alkaline phosphatase sensing," *Journal of Analysis and Testing*, vol. 3, no. 3, pp. 228–237, 2019.
- [9] H. Cheng, S. Lin, F. Muhammad, Y.-W. Lin, and H. Wei, "Rationally modulate the oxidase-like activity of nanoceria for self-regulated bioassays," *ACS Sensors*, vol. 1, no. 11, pp. 1336–1343, 2016.
- [10] L. Yan, H. Ren, Y. Guo et al., "Rock salt type NiO assembled on ordered mesoporous carbon as peroxidase mimetic for colorimetric assay of gallic acid," *Talanta*, vol. 201, pp. 406–412, 2019.
- [11] B. Liu, Z. Huang, and J. Liu, "Boosting the oxidase mimicking activity of nanoceria by fluoride capping: rivaling protein enzymes and ultrasensitive F⁻-detection," *Nanoscale*, vol. 8, no. 28, pp. 13562–13567, 2016.
- [12] F. Chen, M. Bai, K. Cao, Y. Zhao, J. Wei, and Y. Zhao, "Fabricating MnO₂ nanozymes as intracellular catalytic DNA circuit generators for versatile imaging of base-excision repair in living cells," *Advanced Functional Materials*, vol. 27, no. 45, Article ID 1702748, 2017.
- [13] L. Han, J. Shi, and A. Liu, "Novel biotemplated MnO₂ 1D nanozyme with controllable peroxidase-like activity and unique catalytic mechanism and its application for glucose sensing," *Sensors and Actuators B: Chemical*, vol. 252, pp. 919–926, 2017.
- [14] K. Sun, S.-Y. Li, H.-L. Chen, Q.-G. Huang, and Y. Si, "MnO₂ nanozyme induced the chromogenic reactions of ABTS and TMB to visual detection of Fe²⁺ and Pb²⁺ ions in water," *International Journal of Environmental Analytical Chemistry*, vol. 99, no. 6, pp. 501–514, 2019.
- [15] R. Deng, X. Xie, M. Vendrell, Y.-T. Chang, and X. Liu, "Intracellular glutathione detection using MnO₂-nanosheet-modified upconversion nanoparticles," *Journal of the American Chemical Society*, vol. 133, no. 50, pp. 20168–20171, 2011.
- [16] J. Liu, L. Meng, Z. Fei, P. J. Dyson, X. Jing, and X. Liu, "MnO₂ nanosheets as an artificial enzyme to mimic oxidase for rapid and sensitive detection of glutathione," *Biosensors and Bioelectronics*, vol. 90, pp. 69–74, 2017.
- [17] F. Fu, D. D. Dionysiou, and H. Liu, "The use of zero-valent iron for groundwater remediation and wastewater treatment: a review," *Journal of Hazardous Materials*, vol. 267, pp. 194–205, 2014.
- [18] A. Malek, T. Thomas, and E. Prasad, "Visual and optical sensing of Hg²⁺, Cd²⁺, Cu²⁺, and Pb²⁺ in water and its beneficiation via gettering in nanoamalgam form," *ACS Sustainable Chemistry & Engineering*, vol. 4, no. 6, pp. 3497–3503, 2016.
- [19] M. R. Awual, M. Khraisheh, N. H. Alharthi et al., "Efficient detection and adsorption of cadmium(II) ions using innovative nano-composite materials," *Chemical Engineering Journal*, vol. 343, pp. 118–127, 2018.
- [20] R. A. Crane, M. Dickinson, and T. B. Scott, "Nanoscale zero-valent iron particles for the remediation of plutonium and uranium contaminated solutions," *Chemical Engineering Journal*, vol. 262, pp. 319–325, 2015.
- [21] S. Dong, J. Xi, Y. Wu et al., "High loading MnO₂ nanowires on graphene paper: facile electrochemical synthesis and use as flexible electrode for tracking hydrogen peroxide secretion in live cells," *Analytica Chimica Acta*, vol. 853, pp. 200–206, 2015.
- [22] L. Guo, P. Qian, and M. Yang, "Determination of immunoglobulin G by a hemin-manganese(IV) oxide-labeled enzyme-linked immunosorbent assay," *Analytical Letters*, vol. 50, no. 11, pp. 1803–1811, 2017.
- [23] D. He, X. Yang, X. He et al., "A sensitive turn-on fluorescent probe for intracellular imaging of glutathione using single-layer MnO₂ nanosheet-quenched fluorescent carbon quantum dots," *Chemical Communications*, vol. 51, no. 79, pp. 14764–14767, 2015.
- [24] L. Wang, Z. Huang, Y. Liu, J. Wu, and J. Liu, "Fluorescent DNA probing nanoscale MnO₂: adsorption, dissolution by thiol, and nanozyme activity," *Langmuir*, vol. 34, no. 9, pp. 3094–3101, 2018.
- [25] Y. Yuan, S. Wu, F. Shu, and Z. Liu, "An MnO₂ nanosheet as a label-free nanoplatform for homogeneous biosensing," *Chemical Communications*, vol. 50, no. 9, pp. 1095–1097, 2014.
- [26] K. Sun, Q. Luo, Y. Gao, and Q. Huang, "Laccase-catalyzed reactions of 17 β -estradiol in the presence of humic acid: resolved by high-resolution mass spectrometry in combination with 13C labeling," *Chemosphere*, vol. 145, pp. 394–401, 2016.
- [27] S. K. S. Patel, M. Z. Anwar, A. Kumar et al., "Fe₂O₃ yolk-shell particle-based laccase biosensor for efficient detection of 2,6-dimethoxyphenol," *Biochemical Engineering Journal*, vol. 132, pp. 1–8, 2018.
- [28] L. Xu, C. Xu, M. Zhao, Y. Qiu, and G. Sheng, "Oxidative removal of aqueous steroid estrogens by manganese oxides," *Water Research*, vol. 42, no. 20, pp. 5038–5044, 2008.
- [29] S. C. Chien, H. L. Chen, M. C. Wang, and K. Seshiah, "Oxidative degradation and associated mineralization of catechol, hydroquinone and resorcinol catalyzed by birnessite," *Chemosphere*, vol. 74, no. 8, pp. 1125–1133, 2009.

- [30] X. Liu, Q. Wang, H. Zhao, L. Zhang, Y. Su, and Y. Lv, "BSA-templated MnO_2 nanoparticles as both peroxidase and oxidase mimics," *The Analyst*, vol. 137, no. 19, pp. 4552–4558, 2012.
- [31] A. B. Ganganboina and R.-A. Doong, "The biomimic oxidase activity of layered V_2O_5 nanozyme for rapid and sensitive nanomolar detection of glutathione," *Sensors and Actuators B: Chemical*, vol. 273, pp. 1179–1186, 2018.
- [32] A. A. Vernekar, T. Das, S. Ghosh, and G. Muges, "A remarkably efficient MnFe_2O_4 -based oxidase nanozyme," *Chemistry—An Asian Journal*, vol. 11, no. 1, pp. 72–76, 2016.
- [33] E. M. Ko, Y. E. Leem, and H. Choi, "Purification and characterization of laccase isozymes from the white-rot basidiomycete *Ganoderma lucidum*," *Applied Microbiology and Biotechnology*, vol. 57, no. 1-2, pp. 98–102, 2001.
- [34] G. P. Mizobutsi, F. L. Finger, R. A. Ribeiro, R. Puschmann, L. L. D. M. Neves, and W. F. D. Mota, "Effect of pH and temperature on peroxidase and polyphenoloxidase activities of litchi pericarp," *Scientia Agricola*, vol. 67, no. 2, pp. 213–217, 2010.
- [35] J.-S. Lee, M. S. Han, and C. A. Mirkin, "Colorimetric detection of mercuric ion (Hg^{2+}) in aqueous media using DNA-functionalized gold nanoparticles," *Angewandte Chemie International Edition*, vol. 46, no. 22, pp. 4093–4096, 2007.
- [36] W. Li, B. Chen, H. Zhang et al., "BSA-stabilized Pt nanozyme for peroxidase mimetics and its application on colorimetric detection of mercury(II) ions," *Biosensors and Bioelectronics*, vol. 66, pp. 251–258, 2015.
- [37] H. Wei, B. Li, J. Li, S. Dong, and E. Wang, "DNAzyme-based colorimetric sensing of lead (Pb^{2+}) using unmodified gold nanoparticle probes," *Nanotechnology*, vol. 19, no. 9, Article ID 095501, 2008.
- [38] C.-J. Yu, T.-H. Chen, J.-Y. Jiang, and W.-L. Tseng, "Lysozyme-directed synthesis of platinum nanoclusters as a mimic oxidase," *Nanoscale*, vol. 6, no. 16, pp. 9618–9624, 2014.
- [39] B. Liu, X. Han, and J. Liu, "Iron oxide nanozyme catalyzed synthesis of fluorescent polydopamine for light-up Zn^{2+} detection," *Nanoscale*, vol. 8, no. 28, pp. 13620–13626, 2016.
- [40] C.-L. Hsu, C.-W. Lien, S.-G. Harroun et al., "Metal-deposited bismuth oxyiodide nanonetworks with tunable enzyme-like activity: sensing of mercury and lead ions," *Materials Chemistry Frontiers*, vol. 1, no. 5, pp. 893–899, 2017.
- [41] E. I. Solomon, D. E. Heppner, E. M. Johnston et al., "Copper active sites in biology," *Chemical Reviews*, vol. 114, no. 7, pp. 3659–3853, 2014.
- [42] M. Vázquez-González, W.-C. Liao, R. Cazelles et al., "Mimicking horseradish peroxidase functions using Cu^{2+} -modified carbon nitride nanoparticles or Cu^{2+} -modified carbon dots as heterogeneous catalysts," *ACS Nano*, vol. 11, no. 3, pp. 3247–3253, 2017.
- [43] Y. J. Long, Y. F. Li, Y. Liu, J. J. Zheng, J. Tang, and C. Z. Huang, "Visual observation of the mercury-stimulated peroxidase mimetic activity of gold nanoparticles," *Chemical Communications*, vol. 47, no. 43, pp. 11939–11941, 2011.
- [44] S. Zhang, H. Li, Z. Wang et al., "A strongly coupled $\text{Au}/\text{Fe}_3\text{O}_4/\text{GO}$ hybrid material with enhanced nanozyme activity for highly sensitive colorimetric detection, and rapid and efficient removal of Hg^{2+} in aqueous solutions," *Nanoscale*, vol. 7, no. 18, pp. 8495–8502, 2015.
- [45] M. Yan, Y. Lu, Y. Gao, M. F. Benedetti, and G. V. Korshin, "In-situ investigation of interactions between magnesium ion and natural organic matter," *Environmental Science & Technology*, vol. 49, no. 14, pp. 8323–8329, 2015.
- [46] C.-W. Lien, B. Unnikrishnan, S. G. Harroun et al., "Visual detection of cyanide ions by membrane-based nanozyme assay," *Biosensors and Bioelectronics*, vol. 102, pp. 510–517, 2018.
- [47] J. Liu, L. Meng, Z. Fei, P. J. Dyson, and L. Zhang, "On the origin of the synergy between the Pt nanoparticles and MnO_2 nanosheets in Wonton-like 3D nanozyme oxidase mimics," *Biosensors and Bioelectronics*, vol. 121, pp. 159–165, 2018.
- [48] Q. Yang, L. Li, F. Zhao, Y. Wang, Z. Ye, and X. Guo, "Generation of MnO_2 nanozyme in spherical polyelectrolyte brush for colorimetric detection of glutathione," *Materials Letters*, vol. 248, pp. 89–92, 2019.